Separation Science and Technology
Publication details, including instructions for authors and subscription information:
http://www.informaworld.com/smpp/title~content=t713708471

Hydrodynamic Characterization of SPLITT Fractionation Cells

C. Bor Fuh[ab]; Edward M. Trujillo[c]; J. Calvin Giddings[d]
[a] DEPARTMENT OF CHEMISTRY, FIELD-FLOW FRACTIONATION RESEARCH CENTER, SALT LAKE CITY, UTAH [b] Department of Biomedical Engineering, The Cleveland Clinic Foundation, Cleveland, OH [c] DEPARTMENT OF CHEMICAL AND FUELS ENGINEERING, SALT LAKE CITY, UTAH [d] FIELD-FLOW FRACTIONATION RESEARCH CENTER DEPARTMENT OF CHEMISTRY, UNIVERSITY OF UTAH, SALT LAKE CITY, UTAH

To cite this Article Fuh, C. Bor , Trujillo, Edward M. and Giddings, J. Calvin(1995) 'Hydrodynamic Characterization of SPLITT Fractionation Cells', Separation Science and Technology, 30: 20, 3861 — 3876
To link to this Article: DOI: 10.1080/01496399508015148
URL: http://dx.doi.org/10.1080/01496399508015148

SEPARATION SCIENCE AND TECHNOLOGY, 30(20), pp. 3861–3876, 1995

Hydrodynamic Characterization of SPLITT Fractionation Cells

C. BOR FUH*
FIELD-FLOW FRACTIONATION RESEARCH CENTER
DEPARTMENT OF CHEMISTRY

EDWARD M. TRUJILLO
DEPARTMENT OF CHEMICAL AND FUELS ENGINEERING

J. CALVIN GIDDINGS†
FIELD-FLOW FRACTIONATION RESEARCH CENTER
DEPARTMENT OF CHEMISTRY

UNIVERSITY OF UTAH
SALT LAKE CITY, UTAH 84112

ABSTRACT

The efficacy of SPLITT fractionation requires an absence of hydrodynamic mixing between laminae constituting the thin liquid film streaming through a SPLITT cell and it requires structural elements capable of splitting the film evenly along streamplanes. These requirements are examined here by both experimental tests and by a numerical analysis of flow properties near the inlet splitter. The experimental tests, involving dye injection and the injection of pulses of latex particles that may or may not be driven across flow laminae by gravity, show that SPLITT cell performance is close to that of ideal theory at low Reynolds numbers. The computer results verify an absence of mixing under these conditions, but when the Reynolds number and inlet flow asymmetry are both high, vortex motion is found near the inlet splitter edge, suggestive of mixing. The conditions leading to vortex formation are defined. It is shown that tapering the splitter edge suppresses vortex formation.

* Present address: Department of Biomedical Engineering, The Cleveland Clinic Foundation, 9500 Euclid Avenue, Cleveland, OH 44195-5254.
† To whom correspondence should be addressed.

INTRODUCTION

SPLITT fractionation (SF) is a relatively new family of separation techniques primarily (but not exclusively) applicable to macromolecules and particles (1–6). The SF techniques utilize a thin ribbon-shaped flow cell and achieve fractionation by differential transport across the thin (transverse) axis of the cell. Since the cell is only a few hundred μm thick, the separation path (which cannot exceed but may be less than the channel thickness) is extremely short and separative transport is correspondingly rapid. Separation is typically accomplished in only a few minutes. This is a particularly valuable feature for fragile biological species that must be fractionated rapidly to avoid degradation.

The sheet of flowing fluid that carries dissolved or suspended components through the SPLITT cell is divided at both ends by thin flow splitter elements (see Fig. 1). The inlet splitter element allows for the smooth merging of two incoming laminae, one carrying the suspended feed material and the other generally containing only the pure carrier liquid. Differential transport of feed components between the two laminae (after they are brought into contact) then occurs as a result of a transverse driving force or gradient. At the outlet end the liquid sheet is split apart at a predetermined position by a second splitter element, thus producing two substreams that are enriched or depleted in the desired components as a result of the differential transport. This process has been described at considerable length in the literature (1–6).

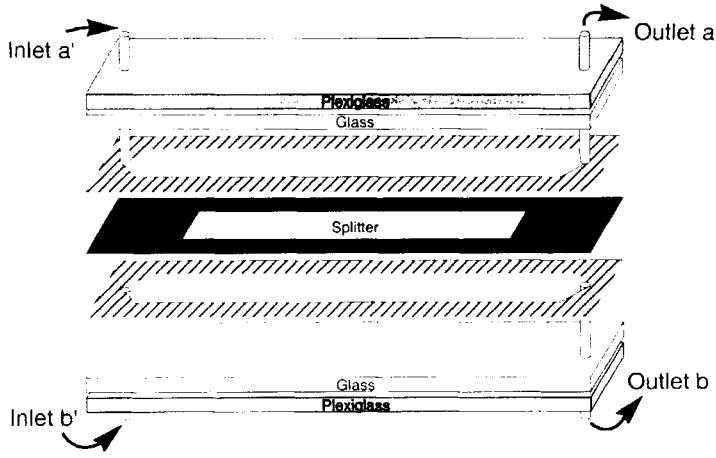

FIG. 1 Structural components of SPLITT cell.

SF is capable of continuous operation and is thus useful as a preparative technique for processing gram, kilogram, or larger quantities of materials. The separation is rigorously controlled by adjusting the two inlet flow rates and the two outlet flow rates and, in some cases, by altering the strength of the field or gradient driving the separative transport. The simplicity of the SPLITT cell leads to rather rigorous theoretical guidelines on the conditions necessary to achieve a given level of separation. Because of its theoretical tractability, the SPLITT cell can also be used for the rapid measurement of transport parameters such as diffusion coefficients (7) and transport-related properties such as particle size and particle size distribution (5).

The principal transverse driving forces used in SPLITT cells include gravity, centrifugation, diffusion, and electrical potential gradients. However, except for moderate curvature in the centrifugal SPLITT cell, the geometry of the different cells is similar with a close resemblance to that depicted in Fig. 1. Therefore, any study that serves to better characterize the behavior of the simple SPLITT cell shown in Fig. 1 will be useful in characterizing the performance of a variety of SF systems and techniques.

The efficacy of SF separation depends on the hydrodynamic integrity of the SPLITT cell. Among other things, effective separation is based on two central requirements: (a) there must be no hydrodynamic mixing across streamplanes and (b) the splitters must be rather perfectly aligned so that they are capable of splitting the film of flowing liquid evenly along a streamplane. Success in fulfilling these requirements is not easy to judge because of the thinness of the cell and the shortness of the transport path; unwanted displacements of a few tens of μm or even a few μm may be difficult to discern but sufficient to interfere with effective separation. Hence it is important to develop various criteria and tests that will define suitable hydrodynamic conditions for separation and assure that the above conditions are met.

In pursuit of the above goals, we have carried out a numerical hydrodynamic study of SPLITT cell flow under a wide range of conditions and we have utilized various empirical tests to examine additional aspects of cell performance. The hydrodynamic study involves an examination of flow in the vicinity of the inlet splitter edge. At this edge, the flow converges sharply, providing an opportunity for significant flow disturbances even at a low Reynolds number. Similar disturbances are expected at the outlet splitter edge.

We have developed and utilized a number of empirical tests to examine SPLITT cell operation. The first is a simple dye injection test which involves introducing dye into one of the inlet substreams. Because of the transparent walls of most cells, the infusion of dye into a cell can be

followed visually, making it possible to recognize in some cases hydrodynamic anomalies as well as significant flaws in the cell assembly and splitter alignment. A more quantitative test (and one that utilizes the same mass transfer process as employed by SF) is carried out by injecting a pulse of monodisperse polystyrene (PS) latex beads into the system and examining the retrieval of the latex material from the two outlets under different conditions. Since latex standards with a defined particle diameter are available in the micron size range, gravity can be used as an effective driving force for transverse transport. The observed retrieval values are then compared with those based on theory, with any significant departure suggestive of hydrodynamic disturbances or structural defects as discussed above.

THEORY

The theory of SPLITT fractionation has been elaborated in a number of publications (2, 4, 8, 9). Here we summarize those aspects of the theory that are essential for the present study.

Separation in a SPLITT cell is controlled by adjustments in component flow rates, as noted earlier. The total flow rate through the cell, $\dot{V}$, is equal both to the sum of the two inlet flow rates and of the two outlet flow rates:

$$\dot{V} = \dot{V}(a') + \dot{V}(b') = \dot{V}(a) + \dot{V}(b) \tag{1}$$

where $\dot{V}(a')$ designates the flow rate of the feed substream a' and where $\dot{V}(b')$, $\dot{V}(a)$, and $\dot{V}(b)$ are the flow rates of b', a, and b, respectively; the substreams b', a, and b are identified by reference to Fig. 1.

The Reynolds number of flow in a thin channel of rectangular cross section having a thickness w and a breadth b can be related to the overall flow rate $\dot{V}$ by

$$\mathrm{Re} = \frac{\langle v \rangle w \rho}{\eta} = \frac{\dot{V}\rho}{b\eta} \tag{2}$$

where $\langle v \rangle$ is the mean fluid velocity and ρ and η are the fluid density and viscosity, respectively (10, 11). At a typical $\dot{V}$ of 6 cm^3/min of a dilute aqueous solution at room temperature through a SPLITT cell with b = 4 cm, the Reynolds number is only 2.5. While flow rates and Reynolds numbers may be one or, in extreme cases, two orders of magnitude higher than the values given in this example, flow along most of the length of the cell is expected to remain laminar under almost all practical circumstances. Flow disturbances around the inlet and outlet splitting edges can occur at lower Reynolds numbers.

We find that the disturbances to flow in the vicinity of the inlet splitter edge is related both to the Reynolds number and to the ratio of flows in the two substreams that are divided by the splitter. Specifically, inlet flow disturbances increase with the inlet flow ratio $r' = \dot{V}(b')/\dot{V}(a')$. This is significant because separation at high resolution requires a very thin feed lamina, which can only be realized if the r' value is high. The tradeoff between resolution (which requires a thin feed lamina and thus a high r') and throughput (which requires a thicker feed lamina) has been described elsewhere (4).

In this paper, inlet flow disturbances are examined as a function of the flow asymmetry A' at the inlet. The inlet asymmetry A' is defined by

$$A' = \frac{\dot{V}(b') - \dot{V}(a')}{\dot{V}(b') + \dot{V}(a')} = \frac{r' - 1}{r' + 1} \tag{3}$$

Values of A' are constrained to the range between -1 and $+1$ but generally fall between $+0.5$ and $+1$.

The exact position of the inlet splitting plane (the surface dividing the two merging flow laminae) is not relevant to ideal SPLITT operation but is important for hydrodynamic calculations. The distance of the inlet splitting plane from the wall at which the feed lamina enters the cell is simply equal to the thickness $w(a')$ of the feed lamina after it contacts the carrier liquid lamina and reaches equilibrium. We have

$$w(a') = w[\sin(\theta/3) + 1/2] \tag{4}$$

where $\sin\theta = -A'$. The position of the outlet splitting plane is calculated in the same manner. The thickness $w(t)$ of the transport lamina is calculated as the distance between the two splitting planes. The volumetric flow rate of the transport lamina is given simply by

$$\dot{V}(t) = \dot{V}(a) - \dot{V}(a') = \dot{V}(b') - \dot{V}(b) \tag{5}$$

Since measurements are made in this paper of the relative retrievals of monodisperse particle standards (i.e., PS latexes) from the two outlet substreams, it is important to give the equations that govern these retrieval values in ideal SPLITT cell operation. In such operation, where a particle is transported at a uniform transverse velocity U from one cell wall toward the other, the particle will migrate across a lamina of volumetric flow rate $\Delta\dot{V}$ as it is carried by flow from the inlet to the outlet splitter. The flow rate $\Delta\dot{V}$ is given by (4)

$$\Delta\dot{V} = bLU \tag{6}$$

where bL is the cell area. When SPLITT cell transport is driven by sedimentation, U equals the product of the sedimentation coefficient s and

acceleration G. Parameter s is related to particle diameter d and the density difference $\Delta\rho$ between the particle and the carrier liquid by the expression $s = \Delta\rho d^2/18\eta$ (4).

The fractional recovery F_a of a monodisperse particle population from outlet a can be calculated from simple equations for ideal SPLITT operation (4). Two limiting models apply. First, if particles sediment to the inlet splitter surface before passing beyond the splitter edge, F_a depends on the relationship of $\Delta\dot{V}$ and $\dot{V}(t)$ as follows:

$$F_a = 0 \quad [\text{for } \Delta\dot{V} > \dot{V}(t)] \tag{7}$$

$$F_a = 1 \quad [\text{for } \Delta\dot{V} \leq \dot{V}(t)] \tag{8}$$

This is referred to as theory 1, descriptive of model 1.

For model 2 the particles arriving at the edge of the inlet splitter are assumed to be homogeneously distributed over the cross section of the feed lamina. In this case F_a is governed by the equations (theory 2)

$$F_a = 1 \quad [\text{for } \dot{V}(t) \geq \Delta\dot{V}] \tag{9}$$

$$F_a = \frac{\dot{V}(a) - \Delta\dot{V}}{\dot{V}(a')} \quad [\text{for } \dot{V}(a) > \Delta\dot{V} > \dot{V}(t)] \tag{10}$$

$$F_a = 0 \quad [\text{for } \Delta\dot{V} \geq \dot{V}(a)] \tag{11}$$

In order to compare the theoretical F_a values given above with experimental values, we use the UV detectors to measure the areas $A(a)$ and $A(b)$ of the latex peaks eluted from outlets a and b, respectively. Experimental F_a values are then calculated from the expression (5)

$$F_a = \frac{\dot{V}(a)A(a)}{\dot{V}(a)A(a) + \dot{V}(b)A(b)} \tag{12}$$

For the detailed hydrodynamic study of the region near the inlet splitter edge, the Navier–Stokes equations governing ideal isothermal fluid flow (no dispersed particles) with constant fluid density were solved numerically using the FLUENT (V3.03) program from Fluent, Inc. (Lebanon, NH). This program uses a finite difference numerical approach and an iterative solution procedure to solve the fundamental equations governing fluid flow and contains built-in graphics packages to display results. A two-dimensional simulation was conducted over an area represented by a small length element (0.1 cm) of the SPLITT cell in the vicinity of the splitter edge and the full thickness (0.0381 cm) of the SPLITT cell. It was assumed that both inlet streams had a fully developed laminar velocity profile (parabolic) prior to the splitter edge. This was confirmed theoreti-

cally. The rectangular elements used for finite difference calculations have a length three times greater than the thickness.

EXPERIMENTAL

The length L, breadth b, and thickness w of the cell or channel used in this study are 20.0, 4.0, and 0.0381 cm (0.015 inch), respectively. The calculated void volume is 3.05 mL. The main components of the SPLITT cell include a stainless steel splitter sandwiched between two Mylar spacers (shown in Fig. 1). Each of these elements is 0.0127 cm (0.005 inch) thick. Triangular cutouts in the ends of the Mylar spacers allow for a smooth transition of the flowstream from the connecting tube into the channel. Two glass plates were used as channel walls enclosing these components. Finally, all these layers were held together by two Plexiglass plates and clamped evenly with bolts.

The carrier liquid used for this study was 0.1% FL-70 detergent (Fisher Scientific, Fair Lawn, NJ) and 0.005% sodium azide (Sigma, St. Louis, MO) in double deionized water. Bromophenol blue (Sigma, St. Louis, MO) was used for the dye injection experiments.

Two UV detectors, one a model SPD-6A from Shimadzu (Kyoto, Japan) and the other a model UV-106 from Linear (Reno, NV), were used in this study. A Teflon rotary valve with a loop volume of 30 μL from Rheodyne (Cotati, CA) was used for sample injection. A Kontron (London, UK) LC pump Model 410 and a QD-0 pump from FMI (Oyster, NY) were used for inlet flows a' and b', respectively. A Minipuls 2 peristaltic pump from Gilson (Middleton, WI) was used to control outlet flow a. Polystyrene latex beads were purchased from Duke Scientific (Palo Alto, CA).

Mylar strips were placed symmetrically on both sides and both ends of the splitter in these studies. Figure 2 shows a top view of the SPLITT

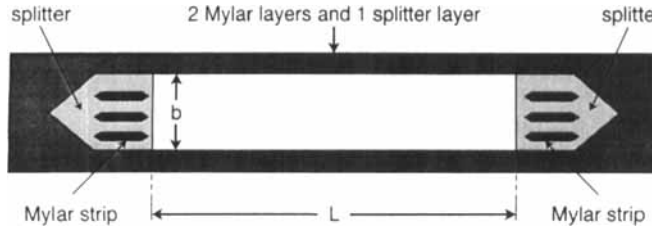

FIG. 2 Top (or bottom) view of SPLITT cell consisting of sandwich (see Fig. 1) of a splitter and two spacers.

cell with the splitter and Mylar strips sandwiched between the two Mylar spacers. The channel was oriented vertically (channel axis was parallel to gravity) when the goal was to avoid gravitational effects on the latex particles and horizontally when gravitational transport was required. All experiments were conducted at room temperature, 24 ± 1°C.

RESULTS AND DISCUSSION

Cell Integrity/Splitter Alignment

A SPLITT cell cannot function properly unless the splitting edges are well aligned. By working at low Reynolds numbers (flow rates) we can distinguish problems arising from splitter misalignment (or other cell imperfections) from those that have a strictly hydrodynamic origin. One such test involves the injection of dye. However, perfusion of dye into the channel usually appears to be quite irregular even when the cell is known to be operating properly. Therefore, the dye test is usually not definitive. However, dye injection can be used in some cases to identify cell defects or even hydrodynamic anomalies.

Injection of PS latex beads can give more quantitative measures of SPLITT cell performance. Two latex tests have been used here. The first is simplest and most rapid and is designed primarily to test splitter alignment. In this test the axis of the SPLITT cell is oriented vertically so that transport will be unaffected by gravity. A thin transport lamina (25 μm) is formed by using slightly asymmetrical inlet and outlet flows: $\dot{V}(a')/\dot{V}(b') = \dot{V}(b)/\dot{V}(a) = 45/55$. The flow rate $\dot{V}$ was 4 mL/min and the Reynolds number was thus only 1.7. A pulse of 5 μm latex beads was injected into feedstream a' and the retrieval factor F_a was obtained by measuring the peak areas of the latex pulses exiting the two outlet substreams a and b using the UV detectors. F_a was calculated from peak areas by means of Eq. (12).

In principle, F_a for the above experiment should be near unity for perfectly aligned splitters because at such a low Reynolds number no transport mechanism exists that will drive a significant fraction of the latex across the 25-μm thick transport lamina. Diffusion, for example, can be calculated from the Stokes–Einstein equation to lead to a displacement of only ~2 μm for 5 μm latex beads, a distance insufficient to lead to significant penetration through the transport lamina. Nonetheless, experimental values of F_a vary from 0.88 to 0.97. While these values are close to unity, they suggest the existence of slight system imperfections.

The second test with latex beads is more realistic because it utilizes normal SPLITT transport. For this test the SPLITT cell is oriented horizontally so that transport is driven by gravity. In the present case, flow

rates were controlled such that $\dot{V}(a') = \dot{V}(b)$ and $\dot{V}(b') = \dot{V}(a)$. The feedstream flow rate $\dot{V}(a')$ was fixed at 0.5 mL/min during this experiment and $\dot{V}(a)$ was allowed to increase systematically. With the increase in $\dot{V}(a)$, the transport lamina thickens and the retrieval factor F_a is expected to increase. The results, using 15 μm PS latex beads, are shown in Fig. 3. The F_a plots based on model 1 (shown as theory 1) and model 2 (theory 2) are shown in the figure. The agreement of the experimental points with these two plots is quite satisfactory; the experimental points are seen to be centered around the theory 1 plot but they have about the same slope as the theory 2 plot. (Particle polydispersity will contribute slightly to the broadening of the F_a plot.) While the agreement of theory and experiment are quite good, a slight departure of the two suggests again that the cell geometry might be slightly imperfect.

Computer Simulation of Flow near Inlet Splitter Edge

The computer program noted earlier was used to obtain solutions to the Navier–Stokes equations in the vicinity of the inlet splitter edge under a number of flow conditions and with different splitter edge configurations. The calculations, like the experiments, apply to a SPLITT cell in which the splitter is centered between the cell walls and has a thickness of $w/3$.

Figures 4 and 5 compare flow properties near the inlet splitter edge at different Reynolds numbers but at the same moderate flow asymmetry

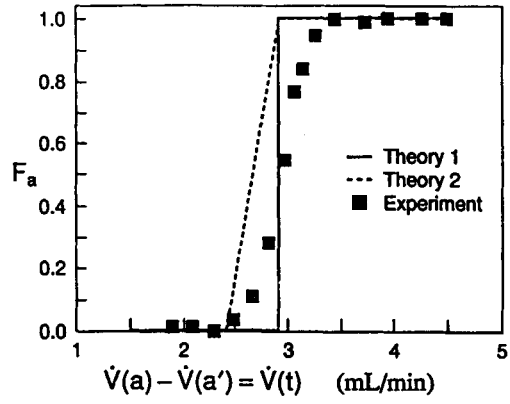

FIG. 3 Examination of SPLITT cell and splitter integrity by comparison of experimental and theoretical retrieval factors with 15 μm polystyrene latex beads subject to transverse gravitational displacement. Flow rate $\dot{V}(a')$ was fixed at 0.5 mL/min and $\dot{V}(a)$ was varied systematically. Other flow rates fixed by $\dot{V}(b) = \dot{V}(a')$, $\dot{V}(b') = \dot{V}(a)$.

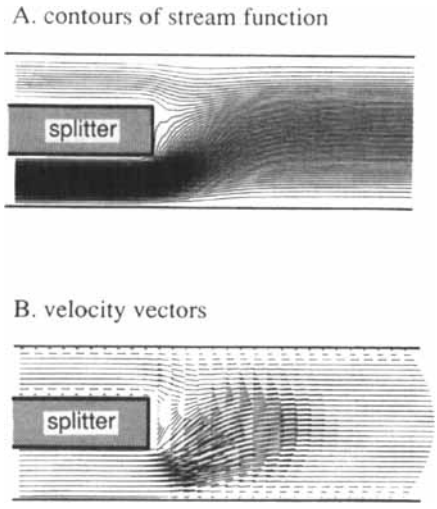

FIG. 4 Stream function contours and velocity vectors from numerical simulation executed in the vicinity of the inlet splitter edge. Parameters: Re = 0.42, $r' = 4$, and $A' = 0.6$.

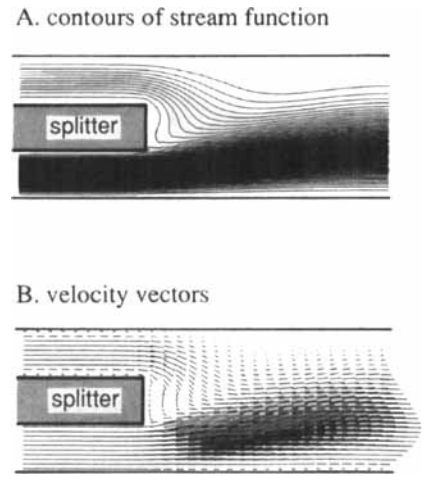

FIG. 5 Flow properties near inlet splitter edge with same parameters as Fig. 4 except Re = 42, equivalent to $\dot{V}$ = 100 mL/min. Stronger inertial effects are evident.

($r' = 4$, $A' = 0.6$). The flow properties are illustrated both by plots of velocity vectors and by contours of the stream function. In Fig. 4 the Reynolds number is 0.42 and in Fig. 5 it is two orders of magnitude higher, 42. These Reynolds numbers correspond to flow rates through the experimental SPLITT cell of $\sim\dot{V} = 1$ and $\dot{V} = 100$ mL/min, respectively. Most SF work is done in this flow-rate range.

Figures 4 and 5 both demonstrate that the flow disturbances induced by the abrupt change in the geometry of the flow space at the splitter edge are attenuated rather rapidly (over the space of a few channel thicknesses) downstream of the disturbance under practical flow conditions. This result is expected for Reynolds numbers well below the turbulent threshold. However, there is a quantitative difference in the two figures reflecting the differences in Reynolds number. In Fig. 4 (Re = 0.42), fluid elements from both inlet substreams change trajectories almost immediately to fill the space immediately downstream of the splitter edge. However, with a Reynolds number 100 times higher (Fig. 5), the fluid from the bottom substream b' (with a flow rate four times higher than that of the upper feedstream a') tends to overshoot the point where the spatial discontinuity is introduced by the splitter edge. The film of liquid corresponding to substream b' accordingly thrusts forward strongly and thus expands much more gradually than the liquid in a' into the body of the SPLITT cell; the combined fluid stream thus fails to establish a steady-state parabolic flow profile in the cell by the time the right-hand margin of the figure has been reached. This observed persistence in flow direction can be ascribed to the relatively large inertial effects associated with the higher Reynolds number. Note that the feed (upper) substream flow, with a local flow rate (prior to reaching the splitter edge) and thus a Reynolds number four times lower than that of the carrier substream, changes direction rather abruptly to fill in the space immediately downstream from the splitter edge.

Although Fig. 5 illustrates that inertial effects clearly influence the details of the transition between flow regimes that occurs at the inlet splitter edge at Re = 42, there is nothing in the calculated results to suggest abnormalities in SPLITT cell behavior or significant deviations from SF theory as presented earlier. The two incoming laminae appear to merge together smoothly at a defined contact surface (the inlet splitting plane) with no indication of hydrodynamic mixing across the surface of contact. The transition zone to reestablish steady-state (parabolic) flow clearly lengthens with the Reynolds number, but Fig. 5 suggests that this transient zone is no longer than about $5w$ at Re = 42. While $5w$ may appear to be a significant distance, it amounts to only 1.9 mm for the experimental cell used in this paper. This distance is less than 1% of the cell length (20 cm). In general, the high aspect ratio (of the order of 10^3) of SPLITT cells will

greatly reduce the effects of any flow transition phenomena as long as mixing does not occur across the contacting boundary.

A large number of computer runs under different flow conditions show that the integrity of the splitting plane becomes compromised as Reynolds numbers are increased, although still held below the turbulent threshold. The appearance of vortex flow (12) suggests that some mixing could occur between incoming laminae. However, vortex activity increases not only with Reynolds number but also with the flow ratio r'. This is illustrated by Fig. 6 in which, by comparison with Fig. 5, Re is reduced from 42 to 21 but r' is increased from 4.0 to 13. The increase in the asymmetry of flow leads to a circular flow pattern as indicated by the figure. (The recirculation of flow is most clearly indicated by the fact that the flow vectors assume a negative direction—unfortunately not shown in the figure—in the upper part of the vortex pattern.)

While both Re and r' in this example are rather large for typical SF operation, these numbers can be exceeded in some practical cases. We have thus elected to examine the possibility that changing the shape of the splitter edge to a more streamlined form will reduce vortex formation. In Fig. 7 we show the results of a computer simulation for a splitter edge that tapers gradually to zero thickness rather than being squared off as in Fig. 6. While the Re and the r' values are identical in Figs. 6 and 7, all indications of vortex activity have disappeared with the change in splitter edge geometry shown in Fig. 7. This result has been verified by numerous other simulations under other flow conditions.

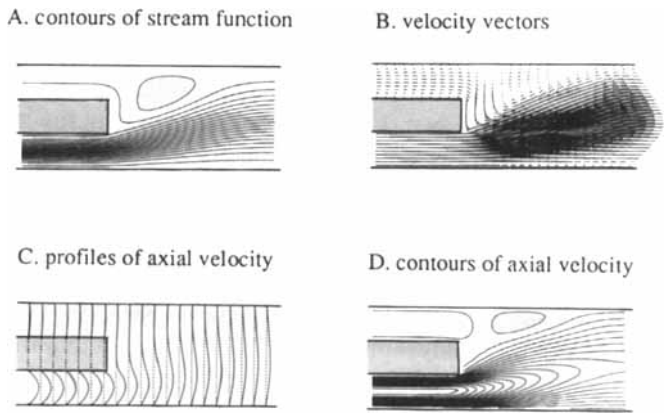

FIG. 6 Details of flow in vicinity of squared off splitter edge. Parameters: Re = 21 ($\dot{V}$ = 50 mL/min), r' = 13, and A' = 0.86.

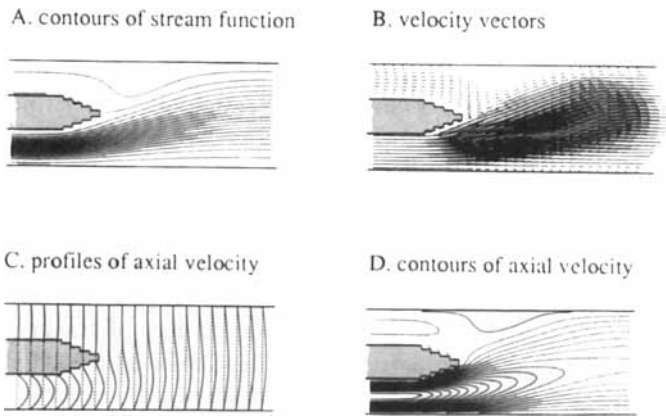

FIG. 7 Details of flow in vicinity of tapered splitter edge. Conditions are the same as reported for Fig. 6.

Figure 8 summarizes the results of a large number of computer simulations which were carried out to define the boundaries of vortex formation with both the squared-off splitter edge and the tapered splitter edge. Boundary points were found by systematically varying Re or r' and noting values for which the vortex first appears in the velocity vector plot.

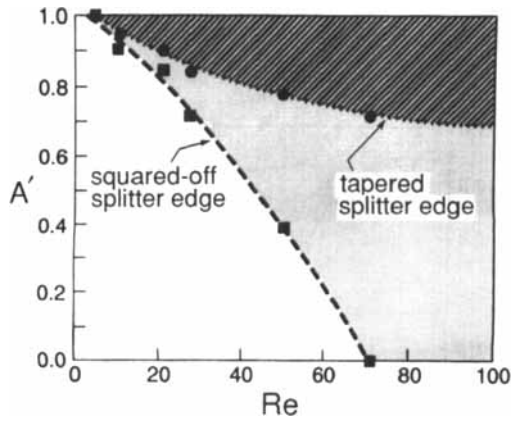

FIG. 8 Regions of vortex formation on plot of asymmetry versus Reynolds number. Boundaries between regions have been determined by the computer simulation points shown. Vortex formation occurs above and to the right of the respective boundaries.

Around 10 computations were required to identify each boundary point; the points were connected to form the boundary lines of Fig. 8. Vortex formation is observed to the right and above the respective lines (i.e., in the shaded areas). This figure illustrates the complementary role of Reynolds number and flow asymmetry in determining the onset of vortex activity.

Because vortexes cannot be directly observed in the thin geometry of the SPLITT cell, no direct proof exists that vortex motion leads to significant mixing between converging laminae. (A direct observation of mixing would require the construction of a scaled-up model of a SPLITT cell with a thickness sufficient to follow the trajectories of tracer particles. Reynolds numbers and asymmetries would need to be adjusted to the same values as utilized here.) However, indirect evidence has accumulated that mixing is associated with well-developed vortex motion. Part of the evidence is shown in Fig. 9. In this figure, values of the retrieval factor F_a as a function of r' are shown for three different Reynolds numbers. At Reynolds numbers of 21 and 27.5, there appears to be a rather abrupt break in F_a at an r' of ~60, which corresponds to $A' = 0.97$. Figure 8 suggests that vortex formation begins somewhat below $A' = 0.9$ at these values of Re, indicating that these experiments involve considerable vortex motion. At Re = 10.5, vortex motion is more borderline. This evidence is suggestive (but not conclusive) that there is a relationship between observed mixing processes in SPLITT cells and well-developed vortex formation.

Additional evidence on mixing resulted from the dye injection experiments. At high Re and r' values, corresponding to well-developed vortex motion, dye injected into the carrier substream (rather than the feed sub-

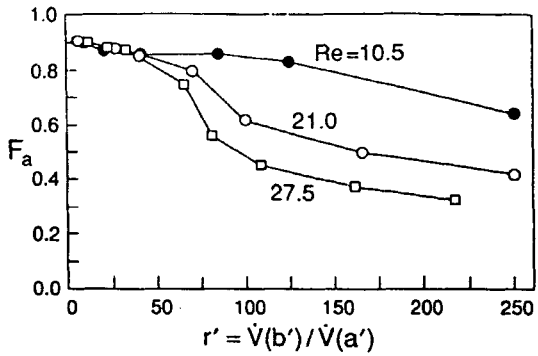

FIG. 9 Plot of retrieval F_a versus inlet flow ratio measured in experiments with 0.596 μm polystyrene latex beads. The thickness of the transport lamina was kept at 24 μm.

stream) is observed to circulate around the splitter edge and back up the feed substream a visible distance from the edge line. While this observation is suggestive of mixing, the upstream penetration of dye is far more pronounced when the Mylar tabs are removed, suggesting that the dye circulation could be related to liquid circulation along the breadth coordinate (which would be inhibited by the tabs) as a consequence of the much larger pressure differences (including a weak pressure gradient along the breadth coordinate) in the carrier stream than in the feed stream. Further evidence is needed to determine the origin of this observation.

CONCLUSIONS

Among various topics explored in this paper, the one of greatest practical interest is the partial delineation of a range of flow conditions in which SPLITT fractionation can be carried out without concern for hydrodynamic disturbances. The ability to achieve effective fractionation under these conditions is supported by experimental results showing that SPLITT cell performance is in reasonable agreement with theory.

The work reported here also begins to answer the question of how far flow conditions can be pushed before fractionation is degraded by hydrodynamic disturbances. A tentative boundary has been found for both squared-off splitter edges and tapered edges such that performance at higher Reynolds numbers and flow asymmetries is suspect. However, we have not significantly tested performance beyond these boundaries. Because it may be possible to achieve a satisfactory level of SPLITT cell performance under more extreme flow conditions than those indicated here, further studies should be done that better compare the results of computer modeling and experimental performance under extreme conditions. Additional work would also be desirable to determine the nature of flow and the development of flow anomalies in the vicinity of the outlet splitter.

ACKNOWLEDGMENTS

This work was supported by Grant CHE-9322472 from the National Science Foundation. We acknowledge Fluent, Inc., for providing the software to the University of Utah.

GLOSSARY

a	outlet at same cell wall as feedstream introduction
a'	feed inlet
A	area of latex peak

A'	inlet flow asymmetry, $(r' - 1)/(r' + 1)$
b	cell breadth
b	outlet opposite to a
b'	carrier inlet
d	particle diameter
F_a	fraction of particle retrieved from outlet a
G	acceleration
L	cell length
r'	inlet flow ratio
Re	Reynolds number
s	sedimentation coefficient
U	transverse velocity
$\langle v \rangle$	mean fluid velocity in SPLITT cell
$\dot{V}$	total volumetric flow rate through SPLITT cell
$\dot{V}(a)$	volumetric flow rate exiting outlet a
$\dot{V}(a')$	volumetric flow rate of feed inlet substream a'
$\dot{V}(b)$	volumetric flow rate exiting outlet b
$\dot{V}(b')$	volumetric flow rate entering inlet b'
$\dot{V}(t)$	volumetric flow rate in transport lamina
w	cell thickness
$w(a')$	thickness of feed lamina
$w(t)$	thickness of transport lamina
$\Delta\dot{V}$	flow rate of lamina crossed by particle with velocity U
η	fluid viscosity
ρ	fluid density

REFERENCES

1. J. C. Giddings, *Sep. Sci. Technol.*, *20*, 749 (1985).
2. S. R. Springston, M. N. Myers, and J. C. Giddings, *Anal. Chem.*, *59*, 344 (1987).
3. S. Levin and J. C. Giddings, *J. Chem. Tech. Biotechnol.*, *50*, 43 (1991).
4. J. C. Giddings, *Sep. Sci. Technol.*, *27*, 1489 (1992).
5. C. B. Fuh, M. N. Myers, and J. C. Giddings, *Anal. Chem.*, *64*, 3125 (1992).
6. C. B. Fuh, M. N. Myers, and J. C. Giddings, *Ind. Eng. Chem. Res.*, *33*, 355 (1994).
7. C. B. Fuh, S. Levin, and J. C. Giddings, *Anal. Biochem.*, *208*, 80 (1993).
8. P. S. Williams, S. Levin, T. Lenczycki, and J. C. Giddings, *Ind. Eng. Chem. Res.*, *31*, 2172 (1992).
9. P. S. Williams, *Sep. Sci. Technol.*, *29*, 11 (1994).
10. R. B. Bird, W. E. Stewart, and E. N. Lightfoot, *Transport Phenomena*, Wiley, New York, 1960.
11. R. D. Belvins, *Applied Fluid Dynamics Handbook*, Van Nostrand Reinhold, New York, 1984.
12. M. Gaster, *J. Fluid Mech.*, *38*, 565–576 (1969).

Received by editor May 8, 1995